RC 22235 November 9, 2001 **Physics**

IBM Research Report

Pressure Instability of bcc Iron

Hong Ma, S. L. Qiu
Department of Physics, Alloy Research Center,
Florida Atlantic University, Boca Raton, FL 33431-0991

P. M. Marcus
IBM T. J. Watson Research Center
P.O. Box 218
Yorktown Heights, NY 10598

Research Division
Almaden - Austin - Beijing - Haifa - India - T. J. Watson - Tokyo - Zurich

Pressure instability of bcc iron

Hong Ma and S. L. Qiu
Department of Physics, Alloy Research Center,
Florida Atlantic University, Boca Raton, FL 33431-0991

P. M. Marcus
IBM Research Division, T. J. Watson Research Center, Yorktown Heights, NY 10598

First-principles total-energy calculations with WIEN97 on ferromagnetic iron in body-cantered tetragonal structure under hydrostatic pressure have shown that the body-centered cubic (bcc) phase exists up to 1500 kbar of pressure. At that pressure a shear constant vanishes and the phase becomes unstable. A body-centered tetragonal (bct) phase is shown to come into existence at 1300 kbar and becomes stable at 1825 kbar and above. This phase may have been observed in the phase diagram of iron above 2000 kbar at high temperature. The pressure dependences of the elastic constants of bcc Fe and of the bct phase are calculated by using the epitaxial Bain path (EBP) of tetragonal Fe generalized to finite pressure and used to define a free energy. The minima at the free energy along the EBP locate the phases; second derivatives of the free energy at the minima give the elastic constants of both the bcc and bct phases as functions of pressure. Minima of tetragonal energies calculated at constant volume are shown to be unreliable for determining stability of a phase.

PACS numbers: 75.10.Lp, 75.50.Bb, 62.20.Dc, 61.50.Ks

I. INTRODUCTON

Under hydrostatic pressure the ferromagnetic (FM) bcc ground state of Fe has decreased magnetization and decreased stability. At the stability-limit pressure p_s this phase of Fe becomes unstable. In previous work, the value of p_s has been estimated as 1000 kbar[1] and as above 2000 kbar[2]. This work fixes the value of p_s at 1500 kbar by evaluating as a function of pressure p the shear constant $C' \equiv (c_{11} - c_{12})/2$ that goes to zero at p_s.

The procedure used to evaluate $C'(p)$ treats FM Fe in body-centered tetragonal (bct) structure at a given p and shows that there is a bcc equilibrium structure at pressures up to p_s. The equilibrium state at each p is found from the epitaxial Bain path (EBP) of FM Fe, which was previously used to find the equilibrium states at $p = 0$ of tetragonal Fe in various magnetic phases[3]. For this work the EBP, which is a special path through tetragonal states that goes through all the equilibrium states, has been generalized to finite p.

The calculation of the EBP finds the total energy E in each tetragonal state on the path. At $p = 0$ the equilibrium states of the magnetic phases of Fe are given by the minima of E. However, at finite p the phases are found from the minima of a free energy (at zero temperature) $G \equiv E + pV$ evaluated along the EBP, where E is the energy per atom and V is the volume per atom. The elastic constant C' at each p is then a second derivative of G at the minima of G taken with respect to a particular shear strain.

The calculations of G for increasing p show that before the pressure reaches p_s, where the bcc minimum of G vanishes, a new noncubic tetragonal minimum of G forms, which persists for $p > p_s$ and becomes stable at $p \geq$ 1825 kbar.

The paper is organized as follows. Section II describes the calculation procedures and shows why the minima of G along the EBP give the equilibrium states at finite p; Section III gives the results of the calculations of G and the elastic constants of the bcc and bct states at p values up to 2000 kbar; Section IV discusses why constant volume calculations fail to determine stability and summarizes the contribution of this work.

II. PROCEDURES

At each point on the tetragonal plane, (coordinate a and c or, equivalently, c/a and $V = ca^2/2$ per atom), the total energy of the body-centered tetragonal lattice $E(a,c)$ can be calculated from first principles. In addition to the energy, the stresses in the basal plane

$$\sigma_1 = \sigma_2 = \frac{1}{ac}\left(\frac{\partial E(a,c)}{\partial a}\right)_c \tag{1}$$

and out of the basal plane

$$\sigma_3 = \frac{2}{a^2}\left(\frac{\partial E}{\partial c}\right)_a \tag{2}$$

can be calculated.

The path on the tetragonal plane called the EBP is found at $p = 0$ for each a by using (2) and the condition $\sigma_3 = 0$. Along the EBP the function $E^{EBP}(a)$ and $V^{EBP}(a)$ are then known, and by construction $(\partial E(a,c)/\partial c)_a = 0$ at every point of the EBP. Then at a minimum of $E^{EBP}(a)$, coordinates a_0, c_0, the derivative of $E(a,c)$ vanishes along the EBP and also along c. Thus the two components of the gradient of $E(a,c)$ on the tetragonal plane must both vanish and a_0, c_0 give a tetragonal energy minimum and corresponds to an equilibrium state in which the stresses given by (1) and (2) vanish.

To generalize the EBP to finite p requires two changes in the procedure used at $p=0$. The first change is to use (2) to find the c at each a at which $\sigma_3=-p$. This procedure finds the EBP at p and the functions $E^{EBP}(a;p)$ and $V^{EBP}(a;p)$. The notation indicates that p is a given parameter, and E^{EBP} and V^{EBP} are functions of a (or c/a) alone at that p.

The second change is to define a free energy at that p (and at zero temperature)

$$G(a,c;p)\equiv E(a,c)+pV(a,c), \tag{3}$$

and look for minima, coordinates a_0, c_0, of

$$G^{EBP}(a;p)\equiv E^{EBP}(a;p)+pV^{EBP}(a;p). \tag{4}$$

At a_0, c_0 using (2) and $p=-\sigma_3$

$$\left(\frac{\partial G(a,c;p}{\partial c}\right)_{a_0,c_0}=\left(\frac{\partial E(a,c)}{\partial c}\right)_{a_0,c_0}+p\left(\frac{\partial V(a,c)}{\partial c}\right)_{a_0,c_0}$$

$$=\sigma_3(a_0,c_0)\frac{a_0^2}{2}-\sigma_3(a_0,c_0)\frac{a_0^2}{2}=0 \tag{5}$$

Since the derivative of $G(a,c;p)$ at a_0, c_0 also vanishes along the EBP, a_0, c_0 give a tetragonal minimum of $G(a,c;p)$ by the same argument used for $p=0$, and

$$\left(\frac{\partial G(a,c;p)}{\partial a}\right)_{a_0,c_0}=\left(\frac{\partial G(a,c;p)}{\partial c}\right)_{a_0,c_0}=0 \tag{6}$$

Furthermore at a_0, c_0 the in-plane stresses σ_1 and σ_2 are given by, using (1), (3) and (6),

$$\sigma_1=\sigma_2=\frac{1}{a_0c_0}\left(\frac{\partial E(a,c)}{\partial a}\right)_{a_0,c_0}$$

$$=\frac{1}{a_0c_0}\left(\frac{\partial G(a,c;p)}{\partial a}\right)_{a_0,c_0}-\frac{p}{a_0c_0}\left(\frac{\partial V(a,c)}{\partial a}\right)_{a_0,c_0}$$

$$=0-p=-p, \tag{7}$$

Thus at a_0, c_0 the system is under hydrostatic pressure p, and $G(a_0,c_0;p)$ is a tetragonal minimum of $G(a,c;p)$ and an equilibrium state under pressure p. The elastic constants at p are then given by second strain derivatives of $G(a,c;p)$ at a_0, c_0, since this open system will try to minimize G rather than E.

The elastic constants of the tetragonal structure at a_0, c_0 with respect to bct orthogonal axes are then given by

$$c_{11}=\frac{2}{c_0}\left(\frac{\partial^2 G(a_1,a_2,c;p)}{\partial a_1^2}\right)_{a_0,c_0}, \tag{8}$$

where only one side of the base is strained, and the tetragonal structure becomes orthorhombic. Also

$$c_{11}+c_{12}=\frac{1}{c_0}\left(\frac{\partial^2 G(a,c;p)}{\partial a^2}\right)_{a_0,c_0}, \tag{9}$$

where the strain preserves the tetragonal structure and

$$c_{66}=\frac{2}{c_0 a_0^2}\left(\frac{\partial^2 G(a,c,\theta_{12};p)}{\partial \theta_{12}^2}\right)_{a_0,c_0,\frac{\pi}{2}}, \tag{10}$$

$$c_{44}=c_{55}=\frac{2}{c_0 a_0^2}\left(\frac{\partial^2 G(a,c,\theta_{23};p)}{\partial \theta_{23}^2}\right)_{a_0,c_0,\frac{\pi}{2}}. \tag{11}$$

The strains in (10) and (11) make the structure monoclinic. It is also useful to introduce the elastic constant Y', a modified Young's modulus, which gives the curvature of the EBP at equilibrium

$$Y'=\frac{1}{c_0}\left(\frac{d^2 G^{EBP}(a;p)}{da^2}\right)_{a_0}=c_{11}+c_{12}-\frac{2c_{13}^2}{c_{33}}. \tag{12}$$

For a cubic structure, $c_{33}=c_{11}$, $c_{13}=c_{12}$ and

$$Y' = \frac{(c_{11} + 2c_{12})(c_{11} - c_{12})}{2c_{11}}. \tag{13}$$

Hence both $C' \equiv (c_{11} - c_{12})/2$ and Y' vanish together for a cubic structure.

The EBPs of FM tetragonal Fe as a function of pressure were found by first-principles total-energy calculations using the full-potential linearized-augmented-plane-wave (FLAPW) method with the Perdew-Burke-Ernzerhof exchange-correlation potential in a generalized-gradient-approximation (GGA)[4]. A plane-wave cutoff R_{MT} Kmax = 9, Gmax = 14 and 300 k-points in the irreducible wedge of the Brillouin zone were used in all the calculations reported here. We found that, although it takes much longer computing time, it is necessary to use R_{MT} = 1.5 a.u. in order to get rid of the ghost bands in the $G^{EBP}(a;p)$ calculations at finite pressure. The k-space integration was done by the modified tetrahedron method[4]. A two-atom tetragonal unit cell with parallel spins was used. All the calculations were highly converged. Tests with larger basis sets and different Brillouin-zone samplings yielded only very small changes in the results.

III. RESULTS

Figure 1 shows the $G^{EBP}(c/a;p)$ curves of FM tetragonal Fe in the vicinity of the bcc point (c/a = 1) at pressures from zero to 2000 kbar, where the reference energy E_0 is the energy per atom in the bcc FM ground state at zero pressure. For clarity, the $G^{EBP}(c/a;p)$ curves at pressures from 300 to 2000 kbar are shifted toward E_0 by 145, 233, 441, 555, 625 and 798 mRy/atom respectively. The $G^{EBP}(c/a;p)$ curve has a minimum at the bcc point at pressures less than 1500 kbar, becomes flat at ~1500 kbar and then has a negative curvature at pressures above 1500 kbar, indicating that the bcc state is unstable at $p \geq 1500$kbar.

Figure 1 also shows that a new bct state at $c/a = 0.877$ develops starting from p = 1300 kbar at which the $G^{EBP}(c/a; p)$ curve has a minimum in addition to the bcc state. With increasing pressure the minimum becomes deeper corresponding to a larger positive curvature. Similar to the bcc state the bct state is also ferromagnetic. Figure 2 shows the local moments of both the bcc and bct states as functions of pressure.

To study the stability of both the bcc and the bct states of FM Fe we have calculated the elastic constants of each state using equations (8) to (13). Figures 3 (a) and (b) show the elastic constants c_{11}, c_{12}, c_{44}, the shear constant C' and the modified Young's modulus Y' of the bcc state as functions of pressure. For a cubic crystal the stability conditions[5] can be given in terms of the three elastic constants; they express the positive definiteness of the strain energy with respect to all small deformations of the lattice. These conditions are

$$c_{11} > |c_{12}|,\ c_{11} + 2c_{12} > 0,\ c_{44} > 0. \tag{14}$$

Figure 3 (a) shows that the bcc state is stable at $p <$ 1500 kbar since all three conditions in (14) are satisfied. Figure 3 (b) shows that both C' and Y' vanish at $p = 1500$ kbar, which is then the precise value of the stability-limit pressure p_s. At $p > p_s$ both C' and Y' become negative, which indicates that the bcc state has become unstable due to the violation of the first stability condition in (14).

The elastic constants c_{11}, c_{12}, c_{44}, and the shear constant C' of the bct state as a function of pressure are shown in Fig. 4. The stability conditions for a tetragonal crystal[5] are

$$c_{11} > |c_{12}|,\ (c_{11} + c_{12})c_{33} > 2\,c_{13}^2,\ c_{44} > 0,\ c_{66} > 0. \tag{15}$$

The first stability condition in (15) is equivalent to $C' > 0$, which is violated at $p <$ 1825 kbar as shown in Fig. 4, indicating that the bct state is unstable at pressures less than 1825 kbar.

Comparison of (15) with (12) reveals that the second stability condition in (15) is equivalent to $Y' > 0$. As mentioned above, the $G^{EBP}(c/a; p)$ curve of the bct state shown in Fig. 1 has a positive curvature corresponding to a positive Y' for $p > 1300$ kbar. Hence the second stability condition in (15) is always satisfied. The third and fourth conditions in (15) are also satisfied since c_{44} and c_{66} of the bct state are positive in the entire region of pressure shown in Fig. 4. The shear constant C' first becomes positive at $p >$ 1825 kbar, when all four of the conditions in (15) are satisfied and the bct state becomes stable at $p >$ 1825 kbar.

For comparison of the present work with previous publications[6-9] we tabulate in Table I the values of the elastic constants c_{11}, c_{12}, c_{44}, the shear constant C' and the modified Young's modulus Y' of bcc FM Fe as a function of pressure. To our knowledge, no elastic constants of the bct state have been reported.

IV. DISCUSSION

Stixrude et al.[1] estimated p_s = 1000 kbar from two $E(c/a)$ curves at constant volume – one at $V = 70$ a.u. corresponding to p = 0 shows a minimum at $c/a = 1$ and one at $V = 50$ a.u. corresponding to $p = 2000$ kbar shows a maximum at $c/a = 1$. Söderlind et al.[2] concluded that $p_s > 2000$ kbar because their $E_V(c/a)$ curve showed a shallow minimum at $c/a = 1$ at V = 7.55Å^3 = 50.9 a.u. corresponding to 2000 kbar (their Fig. 6). Reference 1 missed the shallow minimum at 2000 kbar because the values of c/a used were not spaced closely enough. We have verified the shallow minimum at 2000 kbar. But our Fig. 1 shows clearly that $G^{EBP}(c/a; p)$ at $p = 2000$ kbar has a maximum at $c/a = 1$, indicating $Y' < 0$ and instability. Thus conclusions about stability from minima of $E_V(c/a)$ curves are not reliable.

The formulation here finds elastic constants directly as functions of p, so that the p at which an elastic constant vanishes can be easily evaluated. Also the formulation applies to noncubic phases, hence can be used to find the crossing point of $G(p)$ curves for two phases (the thermodynamic transition), which do not have to be cubic, e.g., one phase can be hcp Fe.

Brown et al.[10] observed experimentally a sound velocity discontinuity in Fe at 2000 kbar and suggested that it was a solid-solid transition at the $\gamma - \varepsilon$ phase boundary. Ross et al.[11] suggested that the shock anomaly at 2000 kbar may be the transition to a new high-pressure solid α' phase with a bcc structure. Söderlind et al.[2] suggested that the α' phase corresponds to a bct state at $c/a = 0.875$ with substantial magnetic moment. However, Söderlind et al.[2] pointed out that they did not know whether this bct state is stable at high pressure. We have shown here from the free energy $G^{EBP}(c/a; p)$ and the elastic constants calculations that the bct state at $c/a = 0.877$ develops starting from p = 1300 kbar and becomes stable at p > 1825 kbar. Therefore, this phase could well be the α' phase observed above 2000 kbar at high temperature, since temperature and vibrational contributions to the free energy could make it the ground state.

ACKNOWLEDGMENTS

The calculations were carried out using the computational resources provided by the MDRCF, which is funded jointly by the NSF and FAU. Hong Ma wishes to thank the financial support from the Department of Physics at Florida Atlantic University. P. M. Marcus thanks IBM for providing facilities as an Emeritus member of the Thomas J. Watson Research Center.

REFERENCE

[1]L. Stixrude, R.E. Cohen, and D.J. Singh, Phys. Rev. B **50,** 6442 (1994).

[2]P. Söderlind, J.A. Moriarty, and J.M. Wills, Phys. Rev. B **53,** 14063 (1996).

[3]S.L. Qiu, P.M. Marcus and Hong Ma, Phys. Rev. B **64,** 104431(2001)

[4]Peter Blaha, Karlheinz Schwarz and Joachim Luitz, *User's Guide for WIEN97*, Vienna University of Technology, 1997; P. Blaha, K. Schwarz, and S.B. Trickey, Comput. Phys. Commun. **59**, 399 (1990).

[5]J. F. Nye, *Physical Properties of Crystals*, Clarendon Press, Oxford (1985).

[6]G.Y. Guo and H.H. Wang, Chinese Journal of Physics, Vol. **38**, No 5, 949 (2000).

[7]J.A. Rayne and B.S. Chandrasekhar, Phys. Rev. Vol. **122**, No. 6, 1714 (1961).

[8]M.W. Guinan and D.N. Beshers, J. Phys. Chem. Solids **29**, 541 (1968).

[9]A.K. Singh, H.K. Mao, Jinfu Shu, and R.J. Hemley, Phys. Rev. Lett. **80**, 2157 (1998).

[10]J.M. Brown and R.G. McQueen, Geophys. Res. Lett. **7**, 533 (1980); J. Geophys. Res. **91**, 7485 (1986).

[11]M. Ross, D.A. Young, and R. Grover, J. Geophys. Res. **95**, 21713 (1990).

TABLE I. Elastic constants c_{11}, c_{12}, c_{44}, Y' and C' of FM bcc Fe as a function of pressure.

	Pressure (kbar)	V_0 (Å^3/atom)	c_{11} (Mbar)	c_{12} (Mbar)	c_{44} (Mbar)	C' (Mbar)	Y' (Mbar)
Present Work	0	11.576	2.852	1.394	0.995	0.729	2.174
	300	10.357	5.656	2.507	1.182	1.575	5.190
	500	9.908	5.372	3.261	1.932	1.056	4.532
	1000	8.857	6.856	4.971	2.850	0.943	4.779
	1500	8.130	6.738	6.772	2.801	-0.017	0
Reference 6	0	11.40	2.79	1.40	0.99	0.69	-------
Reference 7*	0	11.78	2.431	1.381	1.219	0.525	-------
Reference 8*	10	-------	2.62	1.55	1.28	0.54	-------
Reference 9*	46	-------	2.81	1.44	1.23	0.69	-------

* Experimental results

FIGURE CAPTIONS

Figure 1 $G^{EBP}(c/a; p)$ curves in the vicinity of the bcc point (c/a = 1) at pressures of 0, 300, 500, 1000, 1300, 1500, and 2000 kbar. E_0 is the energy per atom in the bcc FM ground state at zero pressure. For clarity, the $G^{EBP}(c/a; p)$ curves at pressures from 300 to 2000 kbar are shifted toward E_0 by 145, 233, 441, 555, 625 and 798 mRy/atom respectively. The solid lines interpolate between the calculated points.

Figure 2 The local magnetic moments of FM Fe in the bcc and bct states as a function of pressure. The solid lines interpolate between the calculated points.

Figure 3 (a) The elastic constants c_{11}, c_{12}, c_{44} of the bcc state of FM Fe as a function of pressure. (b) The shear constant C' and the modified Young's modulus Y' of the bcc state of FM Fe as a function of pressure. Both C' and Y' vanish at $p = 1500$ kbar which is the precise value of the stability-limit pressure p_s. The solid lines interpolate between the calculated points.

Figure 4 The elastic constants c_{11}, c_{12}, c_{44}, c_{66} and the shear constant C' of the bct state of FM Fe at $c/a = 0.877$ as a function of pressure. The change in sign of C' at $p = 1825$ kbar indicates that the bct state becomes stable at $p > 1825$ kbar. The solid lines interpolate between the calculated points.

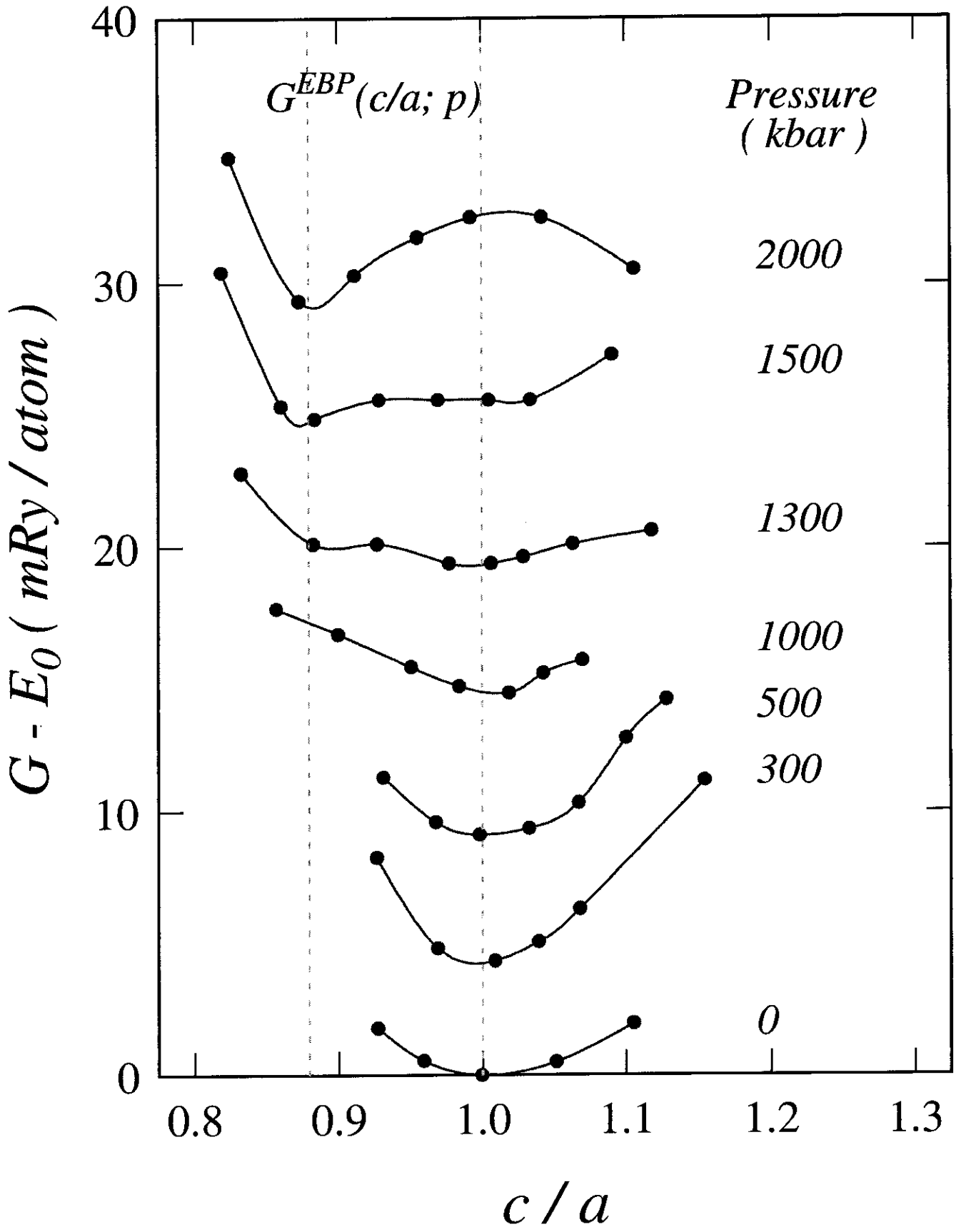

Figure 1 Ma et al.

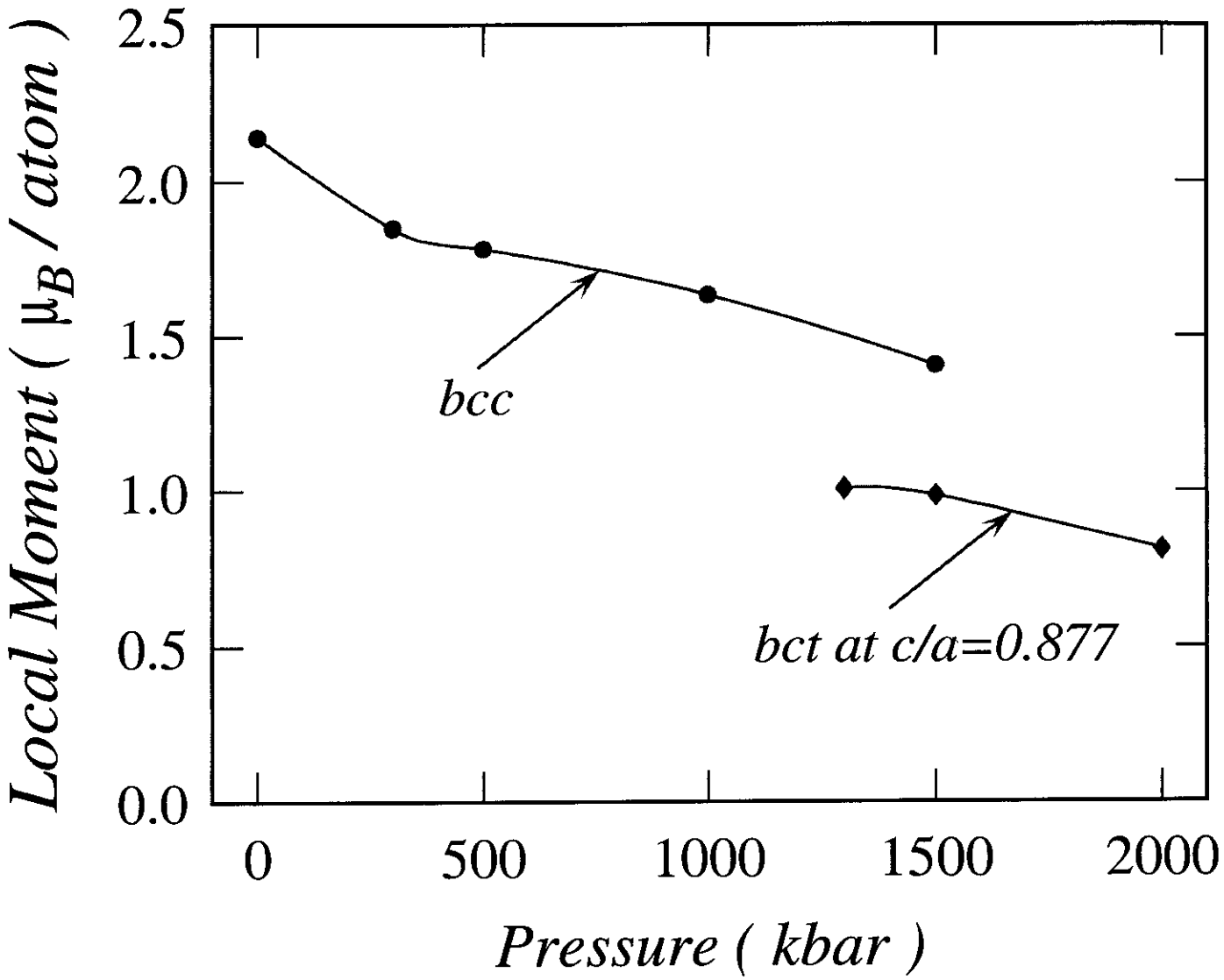

Figure 2 Ma et al.

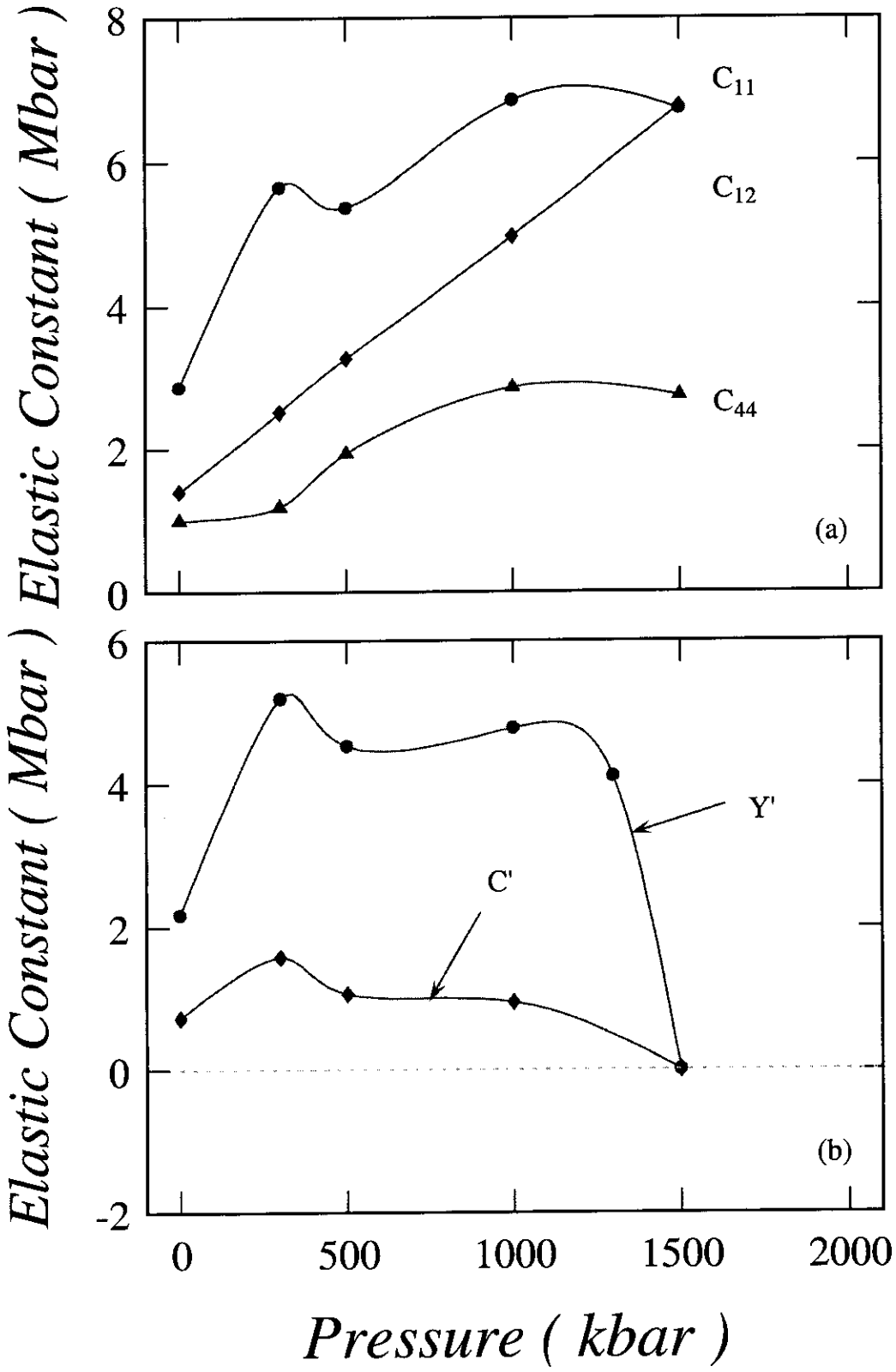

Figure 3 Ma et al.

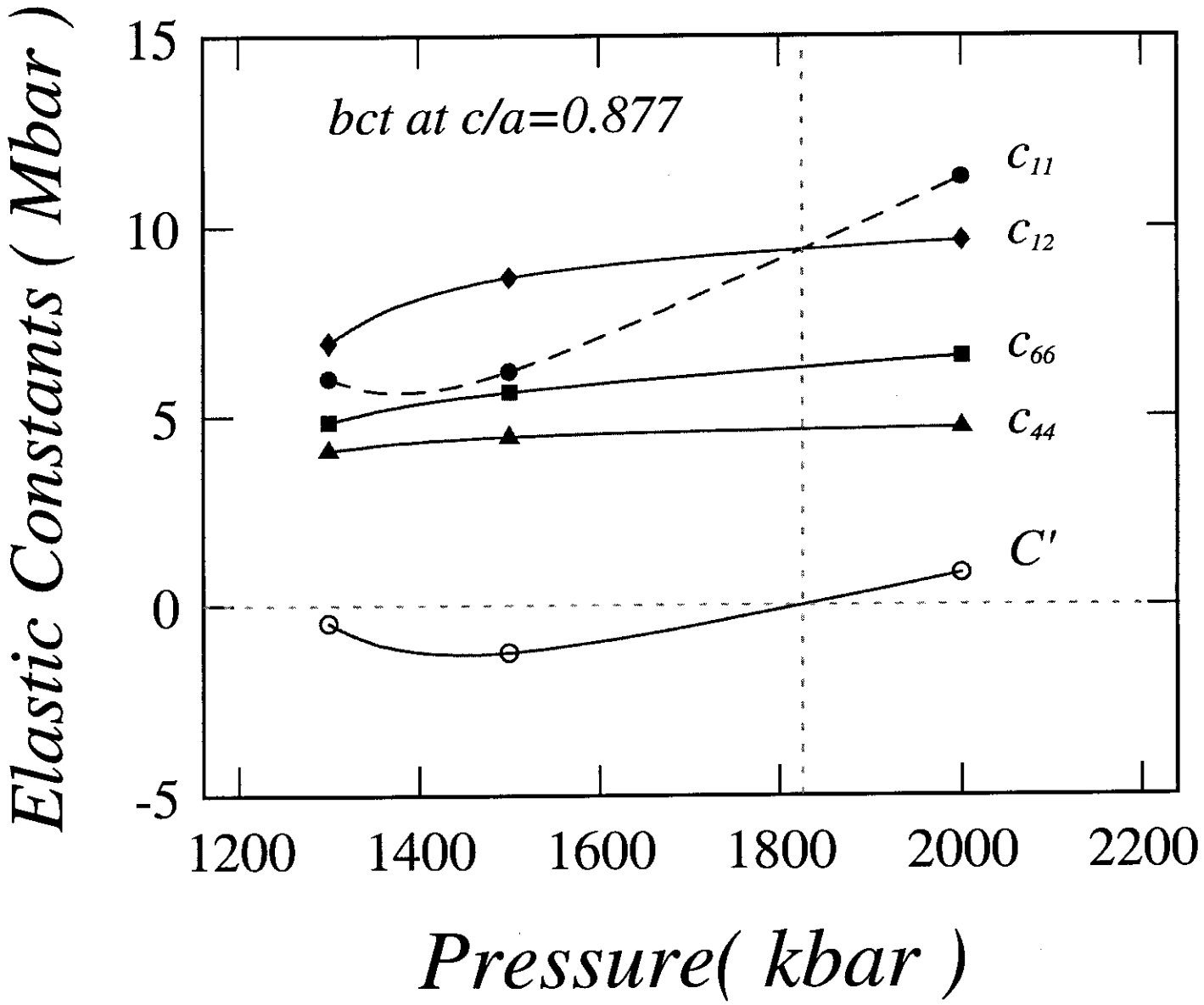

Figure 4 Ma et al.